

Article

Kinetics of Roasting Decomposition of the Rare Earth Elements by CaO and Coal

Shuai Yuan ^{1,2}, He Yang ^{1,2,*}, Xiang-Xin Xue ^{1,2} and Yan Zhou ^{1,2}

¹ School of Metallurgy, Institute of Metallurgy Resources and Environmental Engineering, Northeastern University, Shenyang 110819, China; happyyuanshuai@163.com (S.Y.); xuexx@mail.neu.edu.cn (X.-X.X.); yanzhouchn@gmail.com (Y.Z.)

² Key Laboratory of Liaoning Province for Recycling Science of Metallurgical Resources, Shenyang 110819, China

* Correspondence: yangh@smm.neu.edu.cn; Tel.: +86-130-0243-6218

Academic Editor: Klaus-Dieter Liss

Received: 27 March 2017; Accepted: 6 June 2017; Published: 8 June 2017

Abstract: The roasting method of magnetic tailing mixed with CaO and coal was used to recycle the rare earth elements (REE) in magnetic tailing. The phase transformation and decomposition process were researched during the roasting processes. The results showed that the decomposition processes of REE in magnetic tailing were divided into two steps. The first step from 380 to 431 °C mainly entailed the decomposition of bastnaesite (REFCO₃). The second step from 605 to 716 °C mainly included the decomposition of monazite (REPO₄). The decomposition products were primarily RE₂O₃, Ce_{0.75}Nd_{0.25}O_{1.875}, CeO₂, Ca₅F(PO₄)₃, and CaF₂. Adding CaO could reduce the decomposition temperature of REFCO₃ and REPO₄. Meanwhile, the decomposition effect of CaO on bastnaesite and monazite was significant. Besides, the effects of the roasting time, roasting temperature, and CaO addition level on the decomposition rate were studied. The optimum technological conditions were a roasting time of 60 min; roasting temperature of 750 °C; and CaO addition level of 20% (*w/w*). The maximum decomposition rate of REFCO₃ and REPO₄ was 99.87%. The roasting time and temperature were the major factors influencing the decomposition rate. The kinetics process of the decomposition of REFCO₃ and REPO₄ accorded with the interfacial reaction kinetics model. The reaction rate controlling steps were divided into two steps. The first step (at low temperature) was controlled by a chemical reaction with an activation energy of 52.67 kJ/mol. The second step (at high temperature) was controlled by diffusion with an activation energy of 8.5 kJ/mol.

Keywords: magnetic tailing; REE; CaO roasting; fixing fluorine; kinetics

1. Introduction

Rare earth elements (REE), namely Scandium, Yttrium, and Lanthanides, are irreplaceable strategic resources since they are hailed as “the vitamins of modern industry” and “the treasure house of new materials” [1–3]. The demand for REE has been increasing dramatically in recent years as they are being exploited in various advanced materials and technologies more frequently, such as catalysts, alloys, magnets, optics, and lasers [4,5]. Nevertheless, REE always coexist in nature, and thus, their physical and chemical properties are comparable on account of the high similarity of their atomic structures [6]. Typically, bastnaesite (REFCO₃), monazite (REPO₄), and xenotime are the principal resources of the REE [7,8]. The two largest carbonatite-hosted deposits are the Bayan Obo mine in China and Mountain Pass in USA, and both of them are characterized by rich sources of light REE. The Bayan Obo mine, possessing a polymetallic intergrowth ore of various mineral types, is extremely complex [9–11]. It was originally defined as China’s largest iron ore mine in 1927, with almost 1.5 billion tons of reserves [12]. As the main contributor to the rare earth industry in China [13],

the REE in the Bayan Obo mine was not investigated until decades later. Now, the beneficiation processes of weak magnetic-strong magnetic-flotation are utilized to recover iron resources and REE. The magnetic tailing, which contains a small amount of iron, is subsequently stored in the tailing dam. However, the magnetic tailing not only occupies a large amount of land, but also pollutes the environment. It has become an important factor restricting the sustainability of the Bayan Obo mine [14–16]. The REE in magnetic tailing are crucial resources. Consequently, it is significant for researchers to investigate the properties of the REE in magnetic tailing [17,18].

According to the studies conducted by researchers from all over the world, methods of decomposition to recover the REE such as NaOH roasting [19,20], oxidation roasting [21,22], tailing re-election [23,24], and NH₄Cl roasting [25,26], can be used. The technological process of NaOH involves washing Ca with HCl-washing with water-decomposing with NaOH-washing with water-selective dissolving with HCl-mixed RECl₃ solution. Although these processes do not produce emissions of exhaust gas, they do discharge waste water with fluorine and can be used for high grade REE only. The technological process of oxidation roasting involves oxidation roasting-leaching with HCl-decomposing with NaOH-leaching Ce with HCl. Contrarily, this method has lower costs, the product purity of Ce is relatively low, and it discharge waste includes water and gas. The mechanism of NH₄Cl roasting includes decomposing NH₄Cl into HCl at a certain temperature, and then the HCl will be used to chloridize the REE. This method employed to recover the REE is ecofriendly with no acid or alkali being produced in the processes. In short, while these exploratory studies have made some progress, there are still some disadvantages, such as a lower decomposition rate and a higher gas pollution.

As a crucial strategic resource, the utilization of the REE in magnetic tailing is urgent. In order to develop cleaner production technics, meanwhile improving the recovery rate of the REE, this paper exploits CaO, being an additive, to promote the decomposition of REFCO₃ and REPO₄ and to simultaneously fix the fluorine released from the decomposition of REFCO₃. The addition of CaO will accelerate the decomposition of REFCO₃ and REPO₄ because it is an alkaline oxide. Furthermore, the defluorination reaction will proceed at the same time as the decomposition process of REFCO₃. The fluorine will then be emitted to the atmosphere and cause damage the environment. Therefore, using CaO as an additive can reverse the defluorination reaction to a fluorine-fixing reaction and the fluorine reacts with CaO to form CaF₂ which is left in the slag. Therefore, it will reduce the pollution produced during the process. Besides, if the roasting process is carried out in an oxidation atmosphere, the Ce₂O₃ will be oxidized to CeO₂. However, CeO₂ is harder to leach than Ce₂O₃ during acid leaching. As a result, in this research, coal is used as an additive to prevent Ce₂O₃ oxidizing to CeO₂. Eventually, the kinetics of REFCO₃ and REPO₄ decomposition are studied in order to provide theoretical data for their recovery.

2. Experimental Section

2.1. Experimental Materials

The magnetic tailing used in this research was provided by a Baotou Iron and Steel Concentrator, located at Baotou in China. The coal used in this work was of industrial quality. The chemical composition of the magnetic tailing and coal are given in Tables 1 and 2, respectively. The chemical composition of the magnetic tailing was analyzed using X-ray Fluorescence (XRF). The chemical composition of the coal was analyzed using an industrial analyzer (TRGF-8000, Tianrun Technology, Hebi, China). The CaO was analytically pure.

Table 1. Chemical composition of the rare earth flotation tailing (% , mass fraction).

Fe _{total}	CaO	SiO ₂	F	REO	P ₂ O ₅	BaO	MgO	SO ₃
25.40	21.56	11.26	8.66	6.84	3.10	2.64	2.42	2.42
MnO	Al ₂ O ₃	Na ₂ O	TiO ₂	K ₂ O	Nb ₂ O ₅	ZnO	Cl	Ignition loss
1.60	1.18	0.87	0.56	0.46	0.23	0.06	0.05	10.69

Table 2. Composition of the coal (% mass fraction) where Ad = dry basis ash; Vdaf = volatile dry ash-free basis; Fcad = a fixed carbon content of air dry basis; St,d = dry basis total sulfur.

Ad	Vdaf	Fcad	St,d	Bomb Calorimetric Value/(MJ·kg ⁻¹)
8.78	9.20	82.49	0.30	28.35

2.2. Experimental Methods

2.2.1. Sampling

The particle size distribution was first measured using a laser particle size analyzer (BT9300H, Dandong Bettersize Instrument Co. Ltd., Dandong, China). The results of the particle size analysis are shown in Table 3. According to the result, a particle size smaller than 0.074 mm accounts for 65%. Subsequently, the method of screening is used to obtain the experimental samples smaller than 0.074 mm.

Table 3. Particle size distribution of the sample of magnetic tailing (%).

>149 μm	>74 μm, <149 μm	>58 μm, <74 μm	>38 μm, <58 μm	<38 μm
9.29	25.05	30.71	32.10	2.85

Thereafter, accounting for the proportions, the magnetic tailing was mixed with CaO and coal before the further procedures of mixing, briquetting, and roasting. The detailed processes are described below.

2.2.2. Mixing

Based on the experimental protocol, the coal, magnetic tailing, and CaO were separately weighted. Thereafter, they were placed into a mixing tank and were mixed for five hours using the mixer machine. By mixing the three ingredients, the reaction will be more conducive.

2.2.3. Briquetting

After mixing, the mixture was compressed into briquettes in the briquetting machine (769-40C, Shanghai Jingsheng, Shanghai, China). The diameter and thickness of the briquettes were 30 mm and 10 mm, respectively. The aim of briquetting is to ensure that the mixture has a certain strength and has been properly disseminated. This will make it more conducive to the subsequent operation to accelerate the proceed of the reaction.

2.2.4. Roasting

The briquettes were placed in a graphite crucible sealed with a cap. The graphite crucible was then put into the box resistance furnace (SX_12_16, Shenyang Changcheng, Shenyang, China). The sample was roasted under a certain temperature between 600 °C and 800 °C and the REFCO₃ and REPO₄ were gradually decomposed to rare earth oxides (REO).

2.2.5. Analysis

The roasted samples were analyzed using X-ray powder diffraction (XRD) (PANalytical B.V., Almelo, Netherlands), thermal gravimetric and differential scanning calorimetry (TG-DSC) (Netzsch, Sable, Germany), and scanning electron microscope and energy dispersive spectrometry (SEM-EDS) (Carl Zeiss AG, Jena, Germany). Because the REE can be easily dissolved in acid after decomposition, the roasted samples were dissolved in acid and the content of REE in the residue was then measured. The content of REE was measured with Inductively Coupled Plasma-Atomic Emission Spectrometry (ICP-AES) (Plasma, Beijing, China). The content of fluorine was measured with the method of chemistry titration.

The formulas used to calculate decomposition rate of REFCO_3 and REPO_4 and the fixed fluorine rate are as follows:

$$x_{\text{REFCO}_3 \text{ and REPO}_4} = \frac{m_0 w_0 - m_1 w_1}{m_0 w_0} \times 100$$

$$x_{\text{fluorine}} = \frac{m_1 n_1}{m_0 n_0} \times 100$$

where m_0 is the weight of the magnetic tailing; m_1 is the weight of the roasted sample; w_0 is the content of the REE in the magnetic tailing; w_1 is the content of REE in the roasted sample, which is not decomposed to REO; n_0 is the content of fluorine in the magnetic tailing; and n_1 is the content of fluorine in the roasted sample.

2.2.6. Analytical Facility

The information of the analytical facility used in the experiment is shown in Table 4.

Table 4. Information of the analytical facility.

Analytical Facility	Facility Model and Origin	Purpose
X ray Fluorescence	ZSX 100e, China	Chemical composition of magnetic tailing
industrial analyzer	TRGF-8000, China	Chemical composition of coal
laser particle size analyzer	BT9300H, Dandong Bettersize Instrument Co. Ltd. China	particle size distribution
briquetting machine	shanghai jingsheng, 769-40C, China	briquetting
box resistance furnace	shenyang changcheng, SX_12_16, China	roasting
X-ray powder diffraction	X'Pert Pro, Panalytical, The Netherlands	phase transformation and decomposition process
thermal gravimetric and differential scanning calorimetry	Netsch STA 449F3, Germany	phase transformation and decomposition process
scanning electron microscope and energy dispersive spectrometry	Ultra Plus, Zeiss, Germany	phase transformation and decomposition process
Inductively Coupled Plasma-Atomic Emission Spectrometry	Plasma 1000, China	determining content

3. Results and Discussion

3.1. XRD of Roasted Products

The XRD patterns of the unroasted sample and the samples roasted for 60 min at different temperatures are given in Figure 1. As illustrated in Figure 1a–e, the diffraction peaks of REFCO_3 have completely disappeared in all roasted samples. This means that REFCO_3 decomposed completely when the roasting temperature reached 600 °C and higher than 600 °C. Based on the results, it can be inferred that the decomposition temperature of REFCO_3 is lower than 600 °C. A recent study conducted by Bian et al. [27] states that REFCO_3 is first decomposed to rare-earth oxy-fluorine (REOF). At a low temperature, REOF is the major product of the decomposition of REFCO_3 without any additives. However, the diffraction peaks of REOF are not found in Figure 1. Hence, the REOF then reacts with CaO to form RE_2O_3 and fluorite (CaF_2). This allows Reactions (1) and (2) [27] to proceed. Therefore, it can be found that the addition of CaO can cause REFCO_3 to completely decompose to RE_2O_3 at a low temperature. Meanwhile, the CaO reacts with Fluorine in REFCO_3 to form CaF_2 , and will reduce the pollution caused by fluorine. However, the decomposition temperature of REPO_4 is found to be higher than REFCO_3 . As shown in Figure 1a–e, the diffraction peaks of REPO_4 appear at 600 °C, while disappear in the roasted sample over 650 °C. This indicates that the decomposition temperature of REPO_4 is between 600 °C and 650 °C. Combined with the results of XRD and knowing that there is calcium fluorapatite ($\text{Ca}_5\text{F}(\text{PO}_4)_3$) in the products but no calcium phosphorite ($\text{Ca}_3(\text{PO}_4)_2$),

it can be concluded that CaF_2 contributes to the decomposition reaction of the REPO_4 . The detailed reaction equation is presented as (3) [27]. Furthermore, subsequent to the existence of CeO_2 in the roasted sample when the temperature is between 600°C and 650°C , there are both CeO_2 and Ce_2O_3 in the roasted samples at higher temperatures of 700°C , 750°C , and 800°C . This is major a result, demonstrating that the addition of coal to reactants allows CO to be produced. If the coal is not added to the reactants, Ce_2O_3 will be oxidized to CeO_2 (Reaction (4)). However, CeO_2 is harder to leach than Ce_2O_3 during acid leaching. As a result, in order to pursue subsequent leaching, adding coal to the experiment will generate a reduction of CO gases. When the roasting temperature increases, some CeO_2 will be reduced to Ce_2O_3 , and Reaction (6) will then proceed. Simultaneously, some CeO_2 reacts with Nd_2O_3 to form cerium neodymium oxide ($\text{Ce}_{0.75}\text{Nd}_{0.25}\text{O}_{1.875}$), and thus, there shall also be $\text{Ce}_{0.75}\text{Nd}_{0.25}\text{O}_{1.875}$ in the products. The reaction equation is illustrated in Reaction (5) [27]. From the analysis of XRD, the decomposition products of REFCO_3 and REPO_4 are REO , $\text{Ce}_{0.75}\text{Nd}_{0.25}\text{O}_{1.875}$, and $\text{Ca}_5\text{F}(\text{PO}_4)_3$ in general. Based on the XRD analyses, the conversion may follow the following reactions:

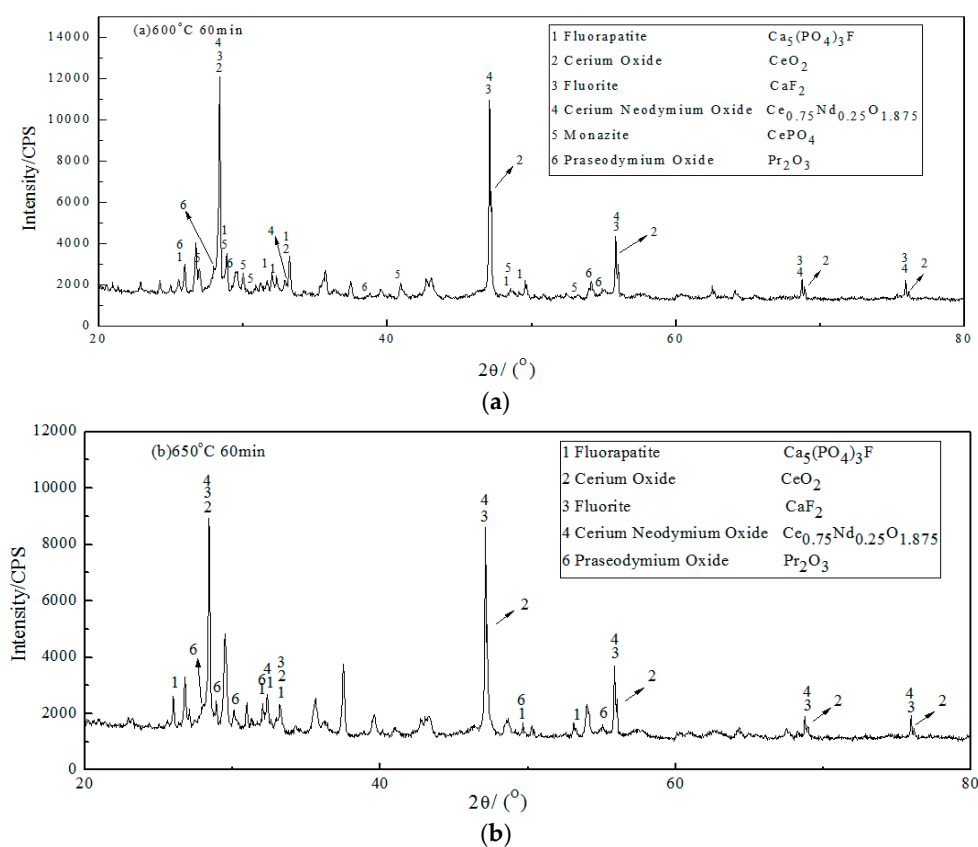
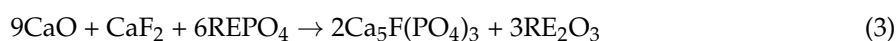
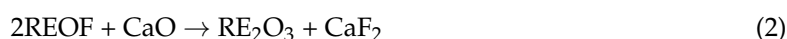


Figure 1. Cont.

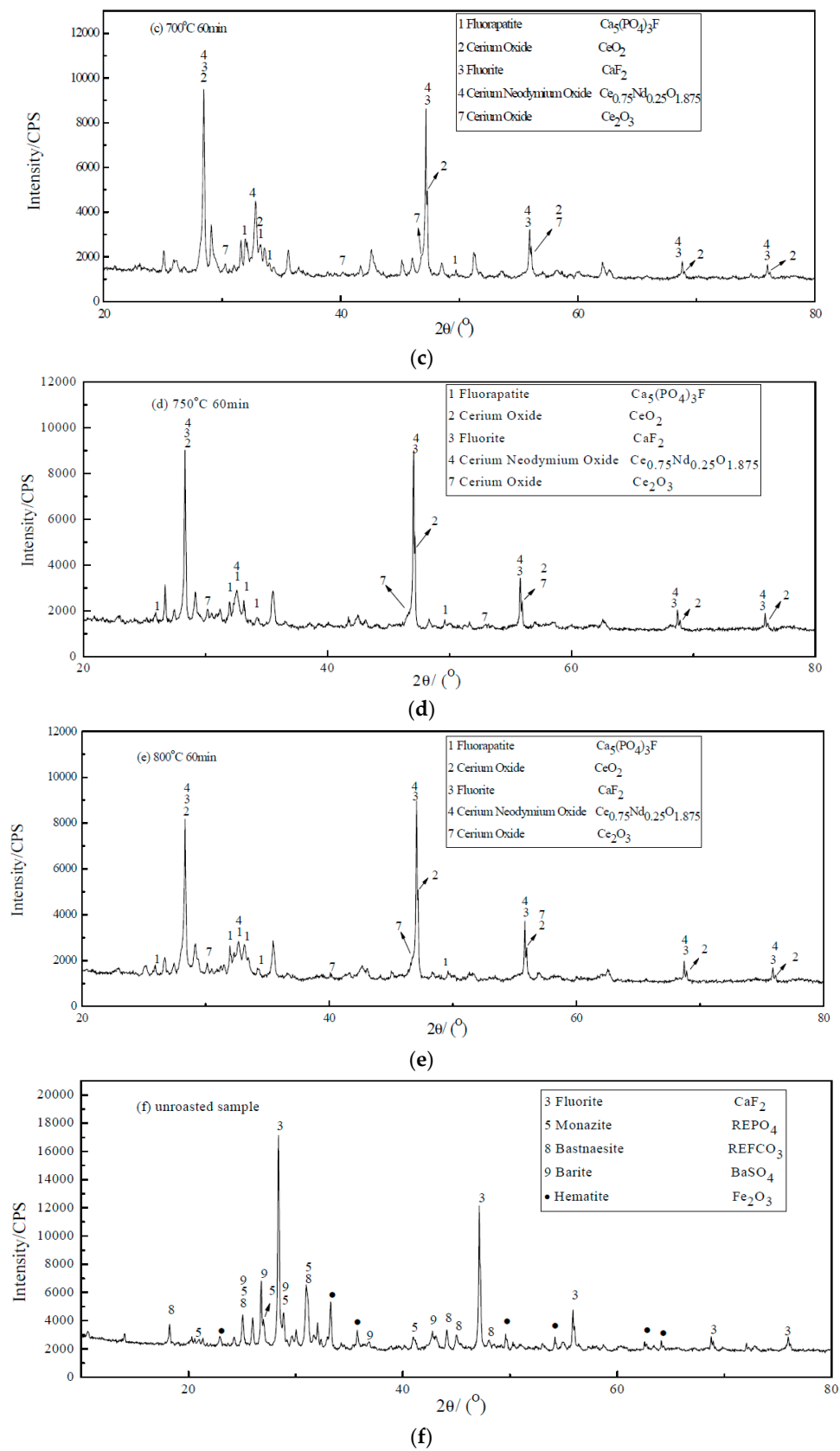


Figure 1. XRD pattern of REE under different conditions. (a) at 600 °C for 60 min; (b) at 650 °C for 60 min; (c) at 700 °C for 60 min; (d) at 750 °C for 60 min; (e) at 800 °C for 60 min; (f) unroasted sample.

3.2. Analysis of TG-DSC

The roasting of magnetic tailing mixed with CaO and coal (rate of mass:1:0.2:0.04 (*w/w/w*)) analyzed by TG-DSC at a heating rate of $10\text{ }^{\circ}\text{C min}^{-1}$ from room temperature to $1100\text{ }^{\circ}\text{C}$ is shown in Figure 2a. The obtained TG-DSC curves imply that the roasting proceeds in two stages. The first stage is from $380\text{ }^{\circ}\text{C}$ to $431\text{ }^{\circ}\text{C}$, with a clear endothermic peak and a weight-loss peak. According to the XRD patterns, the decomposition temperature of REFCO_3 is lower than $600\text{ }^{\circ}\text{C}$. Therefore, it can be inferred that the decomposition temperature of REFCO_3 is between $380\text{ }^{\circ}\text{C}$ and $441\text{ }^{\circ}\text{C}$. To allow a comparison, the TG-DSC curves of the roasting processes of magnetic tailing at a heating rate of $10\text{ }^{\circ}\text{C per min}$ from room temperature to $700\text{ }^{\circ}\text{C}$ (Figure 2b) are studied. Figure 2b demonstrates an endothermic peak and a weight-loss peak between $460\text{ }^{\circ}\text{C}$ and $564\text{ }^{\circ}\text{C}$. In general, Figure 2 shows that the addition of CaO can reduce the decomposition temperature of REFCO_3 . Conversely, Figure 2b demonstrates another endothermic peak and a weight-loss peak between $605\text{ }^{\circ}\text{C}$ and $716\text{ }^{\circ}\text{C}$, which indicates the decomposition of REPO_4 . As the decomposition temperature of REPO_4 is higher than $1900\text{ }^{\circ}\text{C}$ [28] without CaO additives, we can conclude that adding CaO can significantly reduce the decomposition temperature of REPO_4 . In conclusion, we can view that the addition of CaO has a positive effect on decomposing the REPO_4 and REFCO_3 , not only reducing the decomposition temperature, but also completely decomposing to REO.

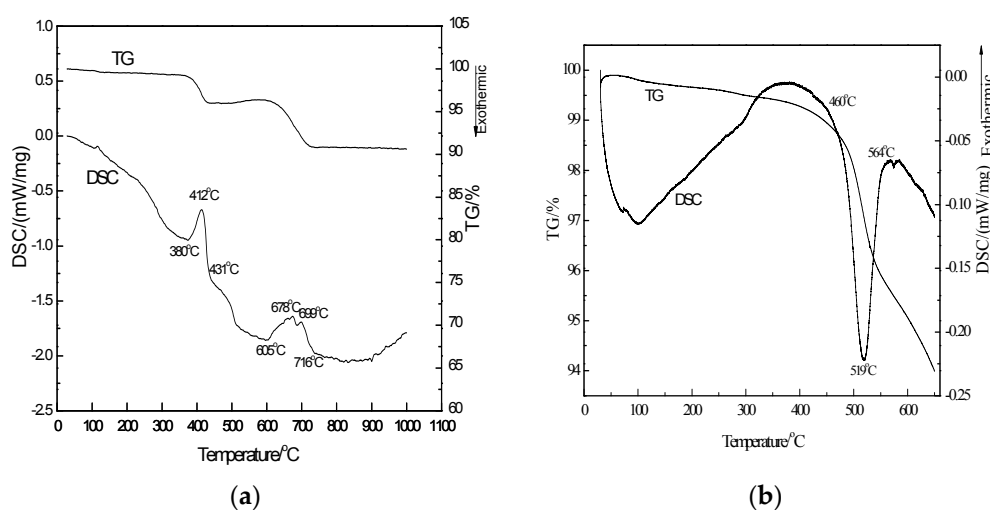


Figure 2. TG-DSC curves of the roasting process at a heating rate of $10\text{ }^{\circ}\text{C min}^{-1}$ (a) magnetic tailing mixed with CaO and coal (b) magnetic tailing.

3.3. Analysis Using SEM-EDS

Figure 3 shows the SEM-EDS results of the examination of the morphology of the unroasted (A) and roasted (B) sample, as well as the analysis of individual REE particles. Spectrum A(a) belongs to a particle consisting of REFCO_3 , A(b) belongs to mixtures of REFCO_3 and REPO_4 , and A(c) and A(d) belong to mixtures of silica (SiO_2) and hematite (Fe_2O_3), respectively. From the morphology of the unroasted sample, we can see that the surface of the REE is smooth and compact with a bright white color, and the REE exhibit particles with an irregular appearance. The REE, SiO_2 , and Fe_2O_3 are coated with each other. Fe_2O_3 and SiO_2 act as substrates and the REE are attached to the surface or collective of the substrate.

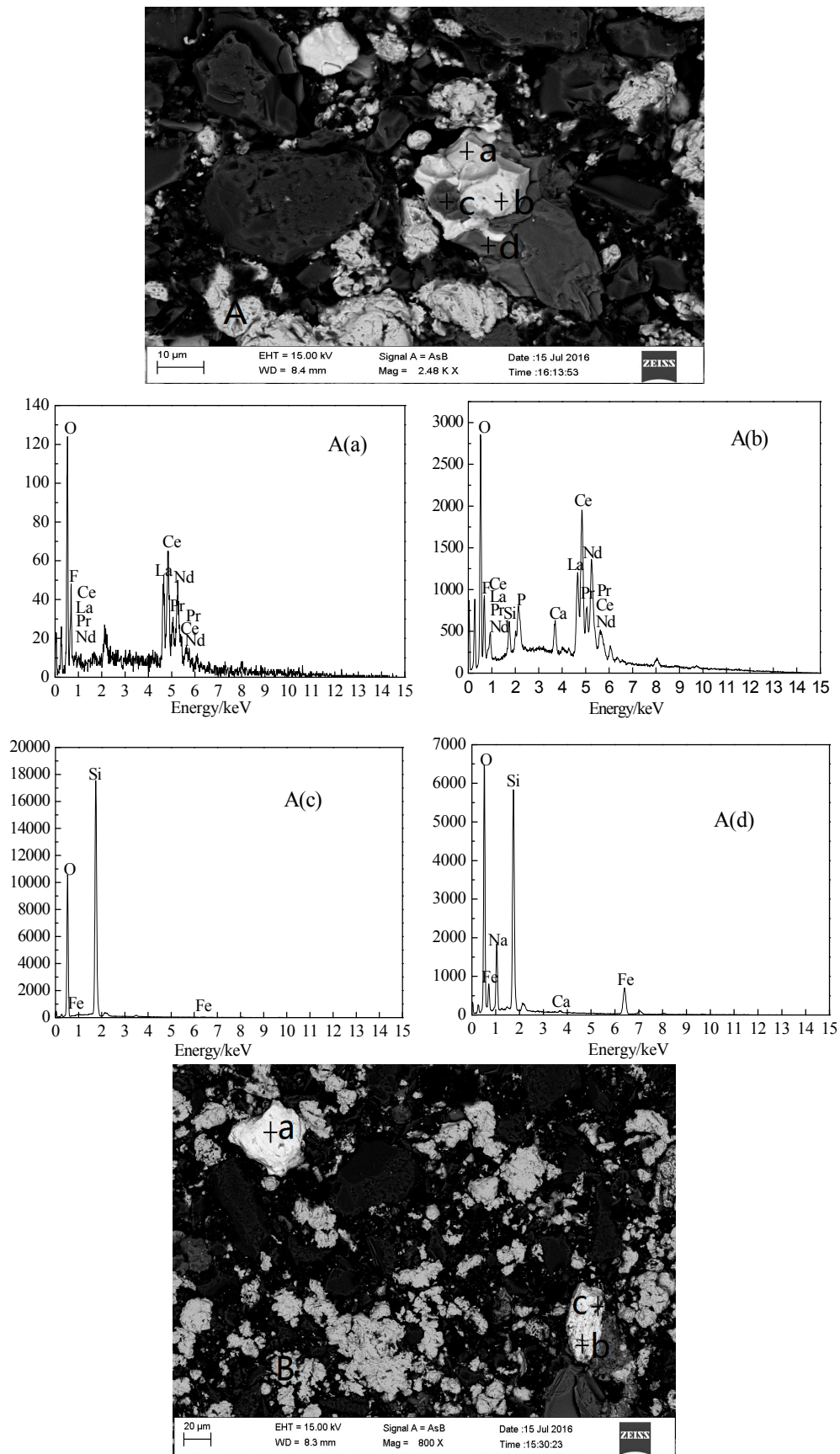


Figure 3. Cont.

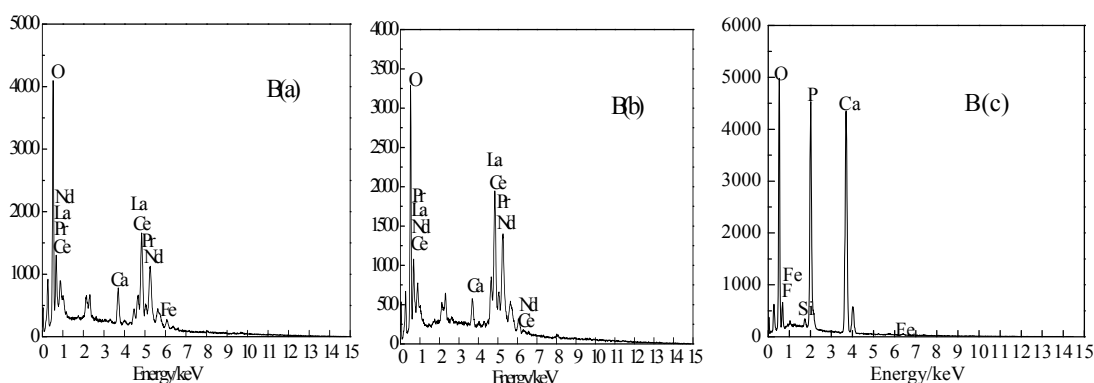


Figure 3. SEM-EDS spectrum of the unroasted sample and roasted sample ((A) unroasted sample; (B) roasted sample for 750 °C at 60 min).

The morphology and element composition of selected particles of the roasted sample are shown in Figure 3B. The spectra B(a), B(b), and B(c) belong to REO, REO, and $\text{Ca}_5\text{F}(\text{PO}_4)_3$, respectively. REFCO_3 and REPO_4 are surely decomposed into REO (Figure 3B). Compared with the unroasted sample, there are more cracks on the surface of the roasted sample due to the gases generated by the decomposition of REFCO_3 , and the morphology of REE seems loose and rough. Meanwhile, the roasted REE samples have different colors (e.g., B(a) is bright white, and B(b) is a mixture of white and black). The EDS analysis shows that B(c) is composed of $\text{Ca}_5\text{F}(\text{PO}_4)_3$ and that B(a) does not contain any $\text{Ca}_5\text{F}(\text{PO}_4)_3$. Therefore, it seems that B(a) consists of the decomposition product of REFCO_3 , while B(b) consists of REFCO_3 and REPO_4 .

3.4. Effect of Roasting Time

Figure 4 shows the results of the decomposition rate of REFCO_3 and REPO_4 with a 20% CaO addition at different roasting times and roasting temperatures ranging from 600 to 800 °C. The decomposition rate of REFCO_3 and REPO_4 increased with the incremental roasting time at all roasting temperatures (Figure 4). However, the growth of the decomposition rate is faster before 60 min and tends to slow down thereafter. Subsequently, when the roasting temperature is lower than 750 °C with a roasting time of less than 30 min, the decomposition rate of REFCO_3 and REPO_4 increases faster with the incremental roasting temperature. When the roasting time is higher than 40 min, the decomposition rate of REFCO_3 and REPO_4 rises faster with the incremental roasting temperature below 700 °C and slows down at higher temperatures. Therefore, it can be found that the decomposition rate at 700 °C for 40 min is a special point, and the decomposition rate increases rapidly at this point. This is a result of the decomposition of REPO_4 . This demonstrates that the REPO_4 decomposes slowly before 40 min and needs a long time to decompose. In conclusion, the decomposition rate of REFCO_3 and REPO_4 reaches its peak after 60 min, providing us with an optimum roasting time of 60 min.

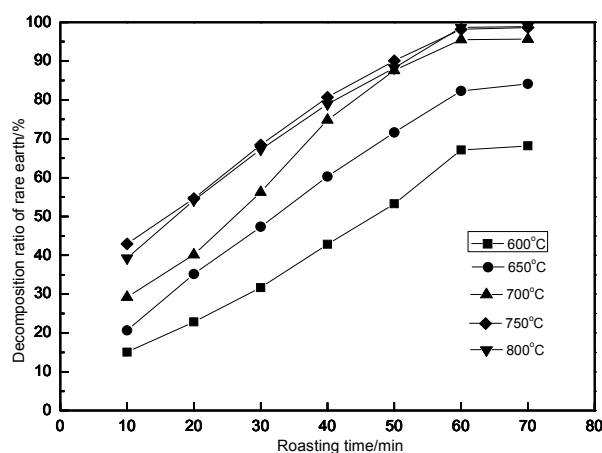


Figure 4. Effect of roasting time on the decomposition rate of REE at different roasting temperatures.

3.5. Effect of Roasting Temperature

With the roasting temperature increasing from 600 to 800 °C for 60 min, a series of experiments are carried out at different levels of CaO addition. The results are shown in Figure 5.

It is observed that the roasting temperature is the most significant factor affecting the decomposition rate of REFCO_3 and REPO_4 (Figure 5). Due to the fact that the decomposition of REFCO_3 and REPO_4 is an endothermic reaction, the decomposition rate increases with the incremental roasting temperature. When the roasting temperature is 600 °C, the decomposition rates are all under 75% at all levels of CaO addition. When the roasting temperature is 650 °C, the decomposition rate is under 85%. At 700 °C, the decomposition rates are all under 95%. However, when the roasting temperature exceeds 750 °C, the decomposition rate is able to reach a level above 95%. The decomposition rate reaches its maximum of 99.87% with a 20% CaO addition and a roasting temperature of 750 °C. Thus, the optimum roasting temperature is 750 °C.

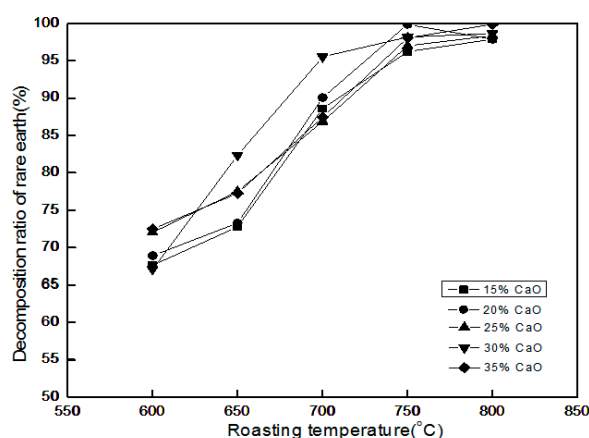


Figure 5. Effect of roasting temperature on the decomposition rate of REE at different levels of CaO addition.

3.6. Effect of CaO Addition

In order to study the effect of the CaO addition level on the decomposition rate of REFCO_3 and REPO_4 , the curve (Figure 6) of the decomposition rate is obtained by adding the CaO addition when the roasting time is 60 min, at a roasting temperature of 750 °C. The decomposition rate does not change significantly with the increased amount of CaO addition (Figure 6). The highest decomposition

rate is 99.87%, when the CaO addition level is 20%. The lowest decomposition rate is 96.21%, when the CaO addition level is 15%. It is found that when the CaO addition level increases from 15 to 20%, the decomposition rate only increases by 3.66%. However, 15% is not chosen as the optimum CaO addition level. This is due to the fact that the decomposition of REFCO₃ and REPO₄ is a solid to solid reaction, and the reaction processes lack liquidity. Thus, to ensure that the REFCO₃ and REPO₄ can make contact with enough CaO, the optimum CaO addition level is 20%.

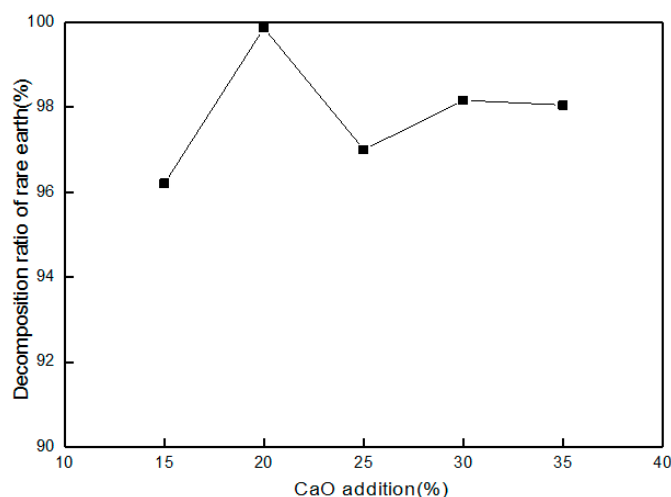


Figure 6. Effect of CaO addition on the decomposition rate of REE.

3.7. Analysis of the Effect of Fluorine-Fixing by CaO

Fluorine is the most important strategic resource, but the discharge of fluorine causes serious pollution. Therefore, it is necessary to recover the fluorine resource. The additive CaO can not only decompose the REFCO₃ and REPO₄, but is also able to bind fluorine. In order to examine the effect of fixing fluorine by CaO, the effect of the roasting temperature on the fix-fluorine rate is studied with a roasting time of 60 min and at a level of 20% of the CaO addition. The results indicate that the fix-fluorine rates are all over 93% with no inconsistent change in the fix-fluorine rate. This shows that the effect of CaO on fluorine fixing is very strong.

3.8. Kinetics Mode of Mixed Rare Earth Tailing's Decomposition Process

The process of magnetic tailing mixing with CaO and coal involves polyphase reactions of solid to solid. The overall reaction rate is determined by the slowest rate-limiting step in the decomposition processes.

To study the decomposition kinetic process of REFCO₃ and REPO₄, the magnetic tailing, CaO, and coal are mixed as a proportion of 100:20:4, with the mixture calcined at different temperatures for different durations. The results of the decomposition rate of REFCO₃ and REPO₄ are shown in Figure 4. The results of Figure 4 are analyzed by Equation (7), which is the equation of the interfacial reaction kinetics model. Although the results of Figure 4 are analyzed by other kinetics models, these models do not produce suitable or ideal results [29].

$$1 - (1 - X)^{1/3} = kt \quad (7)$$

where X is the decomposition rate of rare earth, k represents the rate constants, and t is the reaction time.

The kinetics curves of the decomposition of REFCO₃ and REPO₄ are shown in Figure 7. This process follows the interfacial reaction kinetics model. According to the experimental results of Figure 7, the kinetic constants are derived from Equation (8), also known as the Arrhenius equation, and the results are shown in Figure 8.

$$\ln k = \ln A - \frac{E}{RT} \quad (8)$$

where k is the reaction rate constant, A is the frequency factor, R is the gas constant, T is the temperature, and E is the activation energy.

As shown in Figure 8, the reaction rate controlling steps are divided into two steps. According to the Arrhenius equation (Equation (8)), $-\frac{E}{R}$ is the slope of the straight line in Figure 8. Hence, the activation energy (E) can be calculated from Figure 8 and Equation (8). As a result, the first region (AC segment in Figure 8) has an activation energy of 8.5 kJ/mol. For the second region (CE segment in Figure 8), the activation energy is 52.67 kJ/mol. The activation energy is the main factor which determines the kinetics restrictive conditions. The reaction rate controlling step is a diffusion control when the activation energy is smaller than 13 kJ/mol. It is a mixing control when the activation energy is 20–34 kJ/mol. The chemical reaction controlled the reaction when the activation energy was bigger than 42 kJ/mol. Therefore, the activation energy implies that the reaction rate of the controlling step is a diffusion control mode at high temperature (AB segment in Figure 8) and a chemical reaction control mode at low temperature (BC segment in Figure 8).

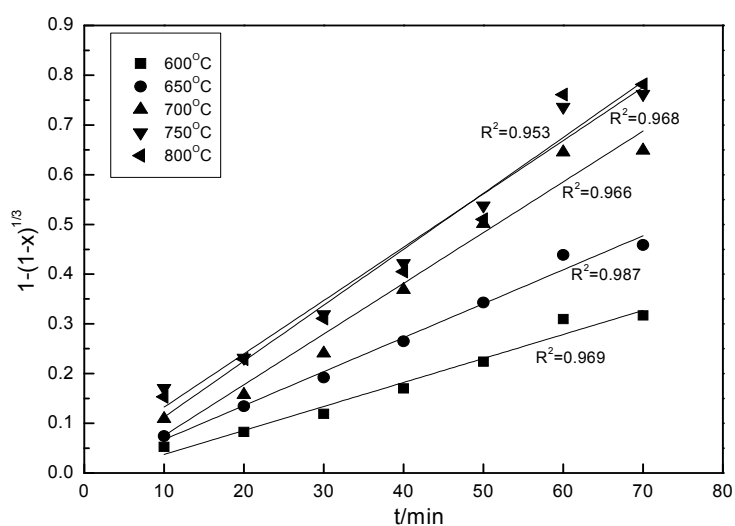


Figure 7. Plots of $1 - (1 - x)^{\frac{1}{3}}$ vs. time at various temperatures.

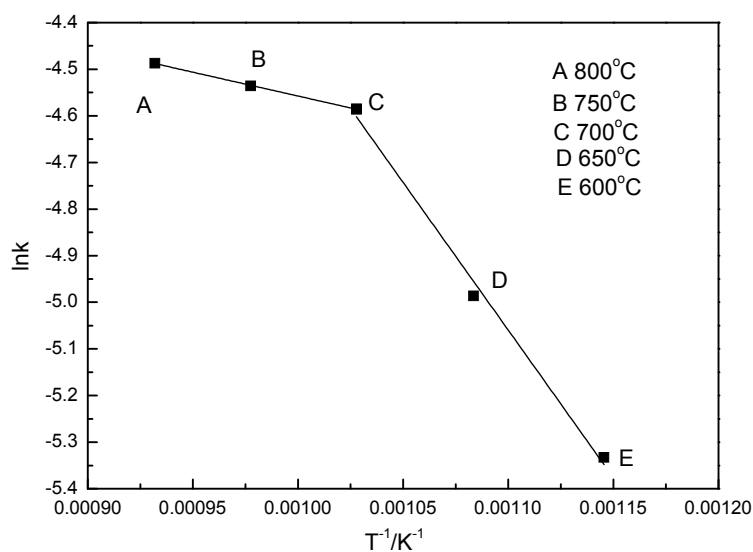


Figure 8. Arrhenius plot for roasting REFCO_3 and REPO_4 .

4. Conclusions

The results show that the decomposition processes can be separated into two steps. The first step from 380 °C to 431 °C is mainly the decomposition of REFCO₃, whereas the second step from 605 °C to 716 °C is mainly the decomposition of REPO₄. The main products are REO, Ce_{0.75}Nd_{0.25}O_{1.875}, Ca₅F(PO₄)₃, and CaF₂. It can also be seen from the SEM-EDS results of the unroasted sample and the roasted samples that the surface of the unroasted sample is relatively smooth and compact, while the surface of the roasted sample is full of cracks. The analysis of the phase transformation and decomposition process proves that the decomposition of magnetic tailing mixing with CaO and coal is an effective method.

The effects of the roasting time, roasting temperature, and the level of CaO addition on the decomposition rates of REFCO₃ and REPO₄ were studied. From these results, the optimum technological conditions are defined as a roasting time of 60 min, roasting temperature of 750 °C, and 20% CaO addition, and the major factors influencing the decomposition rate are the roasting time and roasting temperature. Under the optimum technological conditions, the maximum decomposition rate of REFCO₃ and REPO₄ reaches 99.87%. In addition, the fixing fluorine rate is over 93% in all experiments. Fluorine is fixed in the solid form of CaF₂ and Ca₅F(PO₄)₃ and it reduces the hazardous gas emissions of fluorine.

The kinetics process of the decomposition of REFCO₃ and REPO₄ is consistent with the interfacial reaction kinetics model. The reaction rate controlling steps were divided into two steps. The first step, at a low temperature, is limited by the chemical reaction with an activation energy of 52.67 kJ/mol. The second step, at a high temperature, is controlled by diffusion with an activation energy of 8.5 kJ/mol.

Acknowledgments: National Program on Key Basic Research Project of China (2012CBA01205).

Author Contributions: Shuai Yuan, He Yang, and Xiang-Xin Xue conceived and designed the study; Shuai Yuan and Yan Zhou performed the experiments; Shuai Yuan analyzed the data; He Yang and Xiang-Xin Xue contributed reagents/materials/analysis tools; Shuai Yuan wrote the paper.

Conflicts of Interest: The authors declare no conflict of interest. The founding sponsors had no role in the design of the study; in the collection, analyses, or interpretation of data; in the writing of the manuscript, and in the decision to publish the results.

References

1. Wang, J.L.; Xie, M.Y.; Wang, H.J.; Xu, S.M. Solvent extraction and separation of heavy rare earths from chloride media using nonsymmetric (2,3-dimethylbutyl)(2,4,4'-trimethylpentyl) phosphinic acid. *Hydrometallurgy* **2017**, *167*, 39–47. [[CrossRef](#)]
2. Chen, J.J.; Yang, Q.S. General Survey of Rare Earth Function Materials. *Hunan Nonferr. Met.* **2007**, *23*, 30–33.
3. Eliseeva, S.V.; Bünzli, J.C.G. Rare earths: Jewels for functional materials of the future. *New J. Chem.* **2011**, *35*, 1165–1176. [[CrossRef](#)]
4. Jun, F.; Kazuya, T.; Naoko, W.; Yoshio, T. Simultaneous recovery and separation of rare earth elements in ferromanganese nodules by using *Shewanella putrefaciens*. *Hydrometallurgy* **2016**, *166*, 80–86.
5. Jordens, A.; Cheng, Y.P.; Waters, K.E. A review of the beneficiation of rare earth element bearing minerals. *Miner. Eng.* **2013**, *41*, 97–114. [[CrossRef](#)]
6. Xu, G.X. *Rare Earths*, 2nd ed.; Metallurgical Industry Press: Beijing, China, 1995.
7. Radhika, S.; Nagaphari Kumar, B.; Lakshmi Kantam, M.; Damachandra Reddy, B. Solvent extraction and separation of rare-earths from phosphoric acid solutions with TOPS99. *Hydrometallurgy* **2011**, *110*, 50–55. [[CrossRef](#)]
8. Banda, R.; Jeon, H.; Lee, M. Solvent extraction separation of Pr and Nd from chloride solution containing La using Cyanex 272 and its mixture with other extractants. *Sep. Purif. Technol.* **2012**, *98*, 481–487. [[CrossRef](#)]
9. Huang, X.W.; Li, H.W.; Wang, C.F.; Wang, G.Z.; Xue, X.X.; Zhang, G.C. Development status and research progress in rare earth industry in China. *Rare Met.* **2007**, *31*, 279–288.

10. Cai, Z.L.; Cao, M.L.; Chen, L.P.; Yu, Y.F.; Hu, H.Y. Study on the beneficiation process for recovering rare-earth from the LIMS tailing of HIMS rougher concentrate after magnetizing roasting in Baogang concentrator. *Metalmine* **2009**, *7*, 155–157.
11. Wang, Y.; Yu, X.L.; Shu, Y.; Wang, Z.C. Extraction of rare earths from mixed bastnaesite-monazite of concentrate by carbochlorination reaction. *Nonferr. Met.* **2009**, *61*, 68–71.
12. Wu, C. Bayan Obo controversy: Carbonatites versus Iron Oxide-Ca-Au-(REE-U). *Resour. Geol.* **2008**, *58*, 348–354. [[CrossRef](#)]
13. Zhang, P.S.; Tao, K.J.; Yang, Z.M.; Yang, X.M. *Mineralogy and Geology of Rare Earths in China*; Science Press: Beijing, China, 1995; p. 209.
14. Yang, H.; Wu, J.; Xue, X.X.; Zhang, B.; Li, Y. Roasting and leaching process of mixture of rare earth silicates slag and ammonium sulfate. *J. Chin. Soc. Rare Earths* **2015**, *33*, 440–448.
15. Li, Y.; Lin, N.; He, J.G.; Xue, X.X.; Huang, X.W. Leaching of rare earth and preparaten of cryolite from Baotou magnetic tailings. *J. Chin. Soc. Rare Earths* **2012**, *30*, 251–256.
16. Li, Y.; Wang, M.; Huang, X.W. Alumium roasting-acid leaching of rare earth from Baotou magnetic tailings. *J. Chin. Soc. Rare Earths* **2015**, *33*, 81–86.
17. Yu, X.L.; Wang, Z.C.; Han, Y.X.; Gan, H.M.; Liu, J. Study on process of decomposition of Baosteel concentrator tailings by carbothermic chlorination. *Met. Miner.* **2007**, *9*, 113–115.
18. Yu, X.L.; Wang, Z.C.; Han, Y.X.; Zeng, F.W.; Zhang, Q. Extraction of rare earth from Baogang tailings by carbochlorination reaction tailing AlCl_3 as befluorination agent. *Chin. Rare Earths* **2006**, *27*, 30–34.
19. Xu, Y.H.; Liu, H.J.; Cui, J.G.; Meng, Z.J.; Zhao, W.Y.; Li, L.C. Techniques for clean smelting and resource comprehensive recycle of Baotou rare earth concentrates. *J. Chin. Soc. Rare Earths* **2012**, *30*, 632.
20. Lang, X.C.; Yu, X.L. The latest development of Chinese mixed rare earth concentrate processing. *Rare Met. Cem. Carbides* **2009**, *37*, 43–47.
21. Wang, M.H.; Zeng, M.; Wang, L.S.; Zhou, J.H.; Cui, D.L.; Wang, Q.G.; Wen, R.G.; Chen, X.S. Catnlytic leaching process of bastnaesite with hydrochloric. *J. Chin. Soc. Rare Earths* **2013**, *31*, 148.
22. Wang, X.T.; Liu, J.J. Oxidation baking decomposition process for Baotou mixed RE concentrate. *Rare Earth* **1996**, *17*, 6–9.
23. Ji, J.M. Recovery experiment iron and rare earth minerals from tailing of inverse flotation in dressing plant of Baosteel. *Met. Mine* **2013**, *3*, 158.
24. Zhang, Y.; Ma, P.Q.; Che, L.P.; Qian, J.B.; Ma, Y.P.; Ren, J.H. Study on rare earth flotation from Bao Steel's tailings. *Chin. Rare Earths* **2010**, *31*, 93.
25. Shi, W.Z.; Wang, J.Y.; Zhu, G.C. Kinetics on chlorination rare earth of Baotou mixed concentrate after fixed fluorine treatment. *Chin. J. Nonferr. Met.* **2004**, *14*, 1254–1258.
26. Shi, W.Z.; Zhu, G.C.; Hua, J.; Xu, S.M.; Chi, R.A. Recovery of RE from rare earth concentrate with ammonium chloride roasting. *J. Henan Univ. (Nat. Sci.)* **2002**, *32*, 45–48.
27. Bian, X.; Chen, J.L.; Zhao, Z.H.; Yin, S.H.; Luo, Y.; Zhang, F.Y.; Wu, W.Y. Kinetics of mixed rare earths minerals decomposed by CaO with NaCl-CaCl₂ melting salt. *J. Rare Earth* **2010**, *28*, 86–89. [[CrossRef](#)]
28. Sun, X.C.; Wu, Z.Y.; Bian, X.; Gao, B.; Wu, W.Y.; Tu, G.F. Influence of NaCl-CaCl₂ on decomposing monazite with CaO. *J. Rare Earths* **2007**, *28*, 779–782.
29. Luo, S.Y.; Zhang, J.Y.; Zhou, T.P. Models for kinetics analysis of solid-solid reactions and their Applications. *Mater. Rev.* **2000**, *14*, 6–7.

